

## Ag Ion Transport and Deposition in Quartz

H. B. Vanfleet, G. S. Baker, and P. Gibbs

Citation: *Journal of Applied Physics* **34**, 891 (1963); doi: 10.1063/1.1729556

View online: <http://dx.doi.org/10.1063/1.1729556>

View Table of Contents: <http://scitation.aip.org/content/aip/journal/jap/34/4?ver=pdfcov>

Published by the [AIP Publishing](#)

---

### Articles you may be interested in

[Shiny quartz: luminescence in ionimplanted and epitaxially recrystallizing quartz](#)

*AIP Conf. Proc.* **876**, 154 (2006); 10.1063/1.2406025

[Epitaxial crystallization of keV-ion-bombarded quartz](#)

*J. Appl. Phys.* **89**, 3611 (2001); 10.1063/1.1353805

[Solid phase epitaxial regrowth of ion beam-amorphized -quartz](#)

*Appl. Phys. Lett.* **73**, 1349 (1998); 10.1063/1.122159

[Positive Impurity Ion Emission from Quartz](#)

*J. Appl. Phys.* **37**, 2075 (1966); 10.1063/1.1708674

[Ag Ion Migration in Quartz](#)

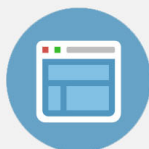
*J. Appl. Phys.* **35**, 2364 (1964); 10.1063/1.1702864

---



## Re-register for Table of Content Alerts

Create a profile.



Sign up today!



## Ag Ion Transport and Deposition in $\alpha$ Quartz\*

H. B. VANFLEET,† G. S. BAKER,‡ AND P. GIBBS

University of Utah, Salt Lake City, Utah

(Received 28 September 1962)

Contact of a negatively charged microprobe to the (0001) face of a silver-backed Madagascar  $\alpha$ -quartz crystal at temperatures between 300–573°C produced four distinct types of visible decorations. The most prominent of these were conducting metallic platelets on the basal plane about 0.4  $\mu$  thick, with surface areas ranging up to the dimensions of the anode. The growth of these platelets appeared to take place only at the periphery, and to be thermally activated with dependence upon field  $\mathcal{E}$  of the form  $\exp[-(H_0 - \beta\mathcal{E})/RT]$ , where  $\beta = 0.32$  kcal/[mole(V/cm)<sup>2</sup>] and  $H_0 = 38$  kcal/mole. Metallic platelets which formed deep within the crystal bulk, having relatively large surface area usually caused the crystal to fracture. The migration of silver through the crystal bulk was observed to take place only in the [0001] direction. Geometric patterns showing the sixfold symmetry of the basal plane were observed to form, at or near the crystal surface, within a fraction of a second upon the application of a negative probe to the (0001) face. Probe currents, both axial and equatorial, were found to be thermally activated with energies between 38 and 39 kcal/mole for conduction not involving the transport of silver ions. Platelet formation in synthetic quartz crystals differed markedly from that for natural quartz. Instead of a conducting metallic platelet, an irregular dendritic growth appeared.

### INTRODUCTION

FOUR component direct currents have been suggested<sup>1,2</sup> to contribute to conduction in quartz: (1) the displacement current (decaying in  $10^{-2}$ – $10^{-1}$  sec); (2) the anomalous current (a small effect dying out 10–15 min after a change in potential); (3) the surge or diffusion current (ascribed to impurity motion, initially large, but decaying in 500–1200 h without external ion source); (4) the steady-state current. Diffusion currents due to  $\text{Li}^+$  and  $\text{Na}^+$  migrating in the [0001] direction were first studied<sup>3</sup> in the late nineteenth century. Agreement with Faraday's law<sup>3</sup> and activation energies of 20 kcal/mole,<sup>4</sup> 17–22 kcal/mole,<sup>5</sup> and 20.6 kcal/mole<sup>5</sup> have been reported for  $\text{Li}^+$ ; 22–25 kcal/mole<sup>5</sup> and 24.0 kcal/mole<sup>2</sup> for  $\text{Na}^+$ ; and 31.7 kcal/mole<sup>5</sup> for  $\text{K}^+$ , where liquid electrolytes<sup>3–5</sup> or nonvolatile salts<sup>2</sup> (up to 350 V) were used as ion source electrodes. It was suggested<sup>5</sup> that the slow process involved either introduction of the ions into the sample, or their removal from it. The activation energies for both surge and high-temperature steady-state currents decrease approximately linearly<sup>4</sup> with the square root of electric field strength. Na and Li migration is decreased 250-fold<sup>6</sup> by  $3 \times 10^{17}$  neutrons/cm<sup>2</sup> neutron irradiation, and activation energy increases with dosage. Cu ions produced<sup>5</sup> an erratic current after

an hour's incubation time as well as copper-colored stains and cracks in the crystal. Spectroscopic evidence was obtained<sup>2</sup> for Mg ion transport from a salt electrode, while Ca, Fe, or Al ions from a salt electrode, and Au, Pt, Al, or Cu from a metal foil gave<sup>2</sup> null results. Material introduced from evaporated Ag film may deposit<sup>7</sup> on (0001) planes in the image<sup>8</sup> of the electrode, or as platelets.<sup>9</sup> Upon cooling, well-developed dendrites or concentric rings may appear.<sup>10</sup> These dissolve if heated above the polymorphic transition temperature, and a line structure forms<sup>10</sup> on subsequent cooling. Cleavage may occur<sup>7</sup> at (0001) precipitates on etching in HF. A breakdown of Si–O tetrahedra in the quartz lattice was suggested<sup>11</sup> to supply the carriers for steady-state current at higher temperatures. O<sub>2</sub> and Si were detected<sup>12</sup> at the respective electrodes of fused quartz subjected to 1 kV/cm at 1000°C. A longitudinal galvanometric effect, suggestive of electronic conduction, was found<sup>13</sup> below 300°C, and its vanishing interpreted<sup>14</sup> to support the ionic conduction mechanism above. In a very careful study 30–450°C, activation energies 35–39 kcal/mole were found<sup>14</sup> for steady axial conduction and 42.9 kcal/mole<sup>15</sup> or 42 kcal/mole<sup>13</sup> for equatorial conduction. A more detailed account of the present experiments may be found in reference 16.

\* This work was supported by the U. S. Office of Naval Research.

† Present address: Department of Physics, Brigham Young University, Provo, Utah. This research formed an essential part of a Ph.D. dissertation in Physics at the University of Utah, Salt Lake City.

‡ Present address: Aerojet-General Corporation, Sacramento, California.

<sup>1</sup> H. E. Wenden, *Am. Mineralogist* **42**, 859 (1957).

<sup>2</sup> J. Verhoog, *Am. Mineralogist* **37**, 637 (1952).

<sup>3</sup> E. Warburg and F. Tegetmeier, *Ann. Physik* **35**, 455 (1888).

<sup>4</sup> P. M. Harris and C. E. Waring, *J. Phys. Chem.* **41**, 1077 (1937).

<sup>5</sup> R. C. Vogel and G. Gibson, *J. Chem. Phys.* **18**, 490 and 1094 (1950).

<sup>6</sup> J. Kirton and E. W. J. Mitchell, *The J. J. Thomson Physical Laboratory, The University of Reading, Reading, England* (preprint).

<sup>7</sup> E. V. Tzinzerling, *J. Tech. Phys. (U.S.S.R.)* **12**, 552 (1942).

<sup>8</sup> F. K. Drescher-Kaden and G. Böttcher, *Naturwissenschaften* **42**, 341 (1955).

<sup>9</sup> H. H. Pfenninger and F. Laves, *Naturwissenschaften* **47**, 276 (1960); **48**, 22 (1961).

<sup>10</sup> J. Van Keymeulen, *Naturwissenschaften* **44**, 489 (1957).

<sup>11</sup> A. F. Joffe, *The Physics of Crystals* (McGraw-Hill Book Company, Inc., New York, 1928).

<sup>12</sup> J. Lietz and W. Münchberg, *Naturwissenschaften* **44**, 487 (1957).

<sup>13</sup> P. E. Sarzhevskii, *Dokl. Akad. Nauk S.S.S.R.* **82**, 571 (1952).

<sup>14</sup> J. C. King, "Fundamental Studies of the Properties of Natural and Synthetic Quartz Crystals" (Final Report, Contract DA 36-039, sc-64586, Prepared by The Bell Telephone Laboratories, 10 June 1960).

<sup>15</sup> E. G. Rochow, *J. Appl. Phys.* **9**, 664 (1938).

<sup>16</sup> H. B. Vanfleet, Ph.D. thesis, University of Utah, Salt Lake City (1961). See also H. B. Vanfleet, G. S. Baker, and P. Gibbs,

### EXPERIMENTAL TECHNIQUE

The combined microscope and manipulation stage was a modified Kentron microhardness tester equipped with a Bausch and Lomb metallographic microscope with 20-mm objective. Above the microscope eyepiece a split-beam prism and 16-mm Bolex motion picture camera was mounted for recording the visually observed phenomena on film. A spigot in the side of the furnace was arranged so that the furnace tube could be continuously flushed with argon, while in operation, in order to protect the tungsten probe from oxidation at the working temperature. The crystal was spring-mounted in a holder, which in turn plugged into an Amphenol connector socket. The connector was mounted on a heavy metal block which was free to slide on a smooth table rigidly attached to the microhardness tester frame. This made it possible to insert the crystal into the furnace tube without making any physical contact with the furnace proper, and insured very high resistance leakage paths between the metallic film on the crystal and the probe. The microprobes for this experiment were made by electrolytically etching the tip of a 10-mil tungsten wire to diameters of approximately  $1\ \mu$ . Probe currents were recorded using a Keithley model 610 electrometer and an Esterline Angus recorder. The furnace ( $\frac{3}{4}$ -in.-i.d. morganite tube) was controlled to within about  $5^\circ\text{C}$  by a Wheelco Amplitrol electronic controller.

Problems arising from surface migration of metallic ions<sup>17,18</sup> were overcome by the use of hollow samples of

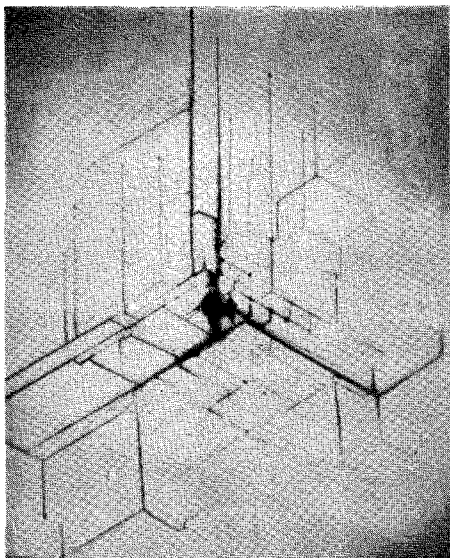


FIG. 1. Geometric pattern produced on the (0001) crystal face by touching a  $-300\text{-V}$  probe to the surface at a temperature of  $470\text{--}530^\circ\text{C}$  (magnification  $\times 90$ ).

Tech. Rept. XV, 15 July 1961, Department of Physics, University of Utah, Salt Lake City, ONR Contract No. N-onr-1288(03), Project No. NR-032-168.

<sup>17</sup> Saul W. Chaikin *et al.*, *Ind. Eng. Chem.* **51**, 299 (1959).

<sup>18</sup> O. A. Short, *Tele-Tech Electron. Ind.* **15**, 64 (1956).

Madagascar, Brazilian, or synthetic<sup>19</sup> quartz about  $\frac{1}{4}\times\frac{1}{4}\times 3$  in., open at one end, and oriented to expose a (0001) face. When Ag contacts were desired inside the hollow, the metal was deposited chemically by the Brashear process. Alternatively, "Gold Bright"<sup>20</sup> was painted in the hollow and fired at  $520^\circ$  for several hours. In this way, a long surface path was provided between the probe (near the closed end) and the Ag contact. In addition, the open end of the quartz sample extended outside the furnace where the temperature was comparatively low. Long narrow z-cut plates of various thicknesses, with metallic electrodes plated on one (0001) face were also used.

### EXPERIMENTAL RESULTS

Four principal types of visible structure were produced by contact of the charged microprobe. These are called "geometric patterns," metallic "platelets," *c*-axis "threads," and center-electrode "spikes." All visible effects discussed below were obtained using chemically deposited Ag in hollow Madagascar quartz samples unless otherwise noted.

"Geometric patterns" (Fig. 1) were rapidly produced at or near the surface on contact of the probe (at about minus 300 V,  $500\text{--}560^\circ\text{C}$ ) with the  $\sim(0001)$  face about 20%–40% of the time. Patterns of the order of 0.1 cm were produced in 0.1 sec. Sometimes they were also produced at points on an expanding metallic platelet.

Metallic "platelets," usually circular (Fig. 2), commenced to grow in a (0001) plane beneath the probe tip shortly after contact, irrespective of whether a geometric pattern had been produced or not. Their resistivity was roughly of the order of  $4\times 10^{-6}\ \Omega\ \text{cm}$ . Blemishes in the film source of Ag were translated along the *c* axis, and imaged in the platelets. It appeared that one could

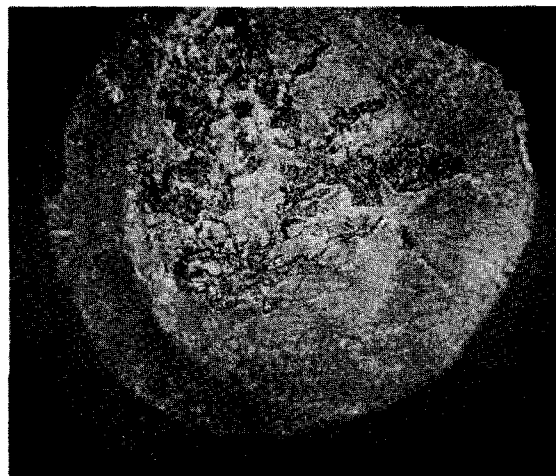


FIG. 2. Typical silver platelet (magnification  $\times 32$ ).

<sup>19</sup> Supplied by Sawyer Research Products, Inc.

<sup>20</sup> Gold in organic suspension. Supplied by the Mach Company, Torrance, California.

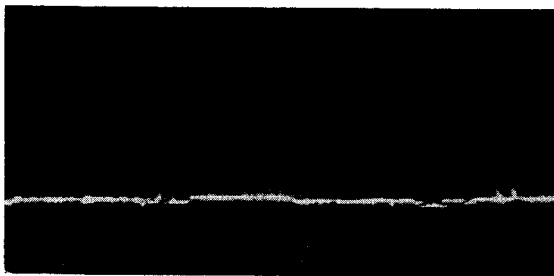


FIG. 3. Platelet edge, showing step in platelet plane and the overall uniformity in thickness (magnification  $\times 1334$ ).

“write his name in silver” inside the quartz. A series of parallel platelets could be grown by contact of the probe with a beveled surface, or by successively reversing the direction of current flow. Figure 3 illustrates a uniform platelet thickness between 0.3 and 0.5  $\mu$ . (Exact measurement was difficult because of light scattering.) Steps of several thousand angstroms can be seen. Figure 4 exhibits a corduroy or stringy platelet surface texture reminiscent of solidification. The platelets tended to avoid crossing lines of a geometrical patterns formed on a previous run (after which the probe was moved).

Straight “threads,” less than 1  $\mu$  in diameter, sometimes extended from platelets along the  $c$  axis toward the Ag source for a hundred microns or so, as in Fig. 5. “Ganglia,” or spheres of about a micron in diameter, often appeared randomly along the threads. Electrical connection between closely spaced neighboring platelets appeared to be established in small regions densely populated with threads. Figure 6 is an example where the platelets are 40  $\mu$  apart.

“Spikes” appeared on the Ag plated hollow about 40 min after a previously probed sample had cooled to room temperature. The spikes tend to lie at  $53^\circ$  to the basal plane, and extend 0.05 cm or less into the crystal. Spikes were not observed when the Ag source was deposited on a carefully polished planar surface. Their orientation is similar to “cracks” etched by Nielson.<sup>21</sup>

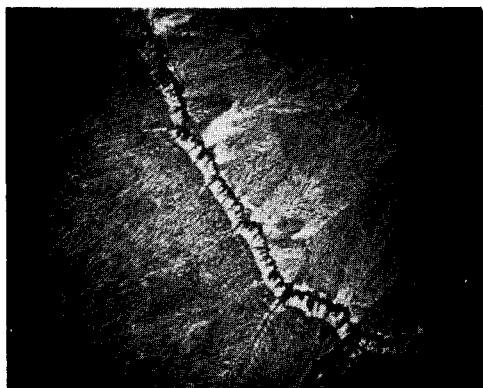


FIG. 4. Corduroy texture of metallic silver platelet surface (magnification  $\times 180$ ).

<sup>21</sup> J. W. Nielson and F. G. Foster, “Unusual Etch Pits in Quartz Crystals” (preprint, The Bell Telephone Laboratories).



FIG. 5.  $c$ -axis threads extending from, and perpendicular to a silver platelet, with attached “ganglia” (magnification  $\times 1500$ ).

Chemical spot tests<sup>22</sup> indicated the presence of Ag in the platelets. Laue back-reflection pictures along the  $c$  axis showed the normal rings expected of Ag foil superimposed in the Laue pattern for quartz, whose spots were distorted. No evidence of single Ag grains could be detected in the Laue pattern, suggesting a grain size less than about 5  $\mu$ . On the other hand, the  $K\alpha_1$  and  $K\alpha_2$  lines were resolved sufficiently to suggest the Ag grain size was greater than 0.1  $\mu$ . Splitting of the quartz spots, suggestive of small angle boundaries up to  $\frac{1}{4}$  degree, was produced by an x-ray beam in the basal plane which intercepted several platelets on adjacent planes. However, no change in the quartz lattice spacing (to 1 part in  $10^4$ ) could be detected on a parallel-plate sample through which 2 mg/cm<sup>2</sup> Ag had passed.

Gross fracture frequently originated at platelet edges. What appeared to be microcracks were often visible extending beyond the platelet, sometimes departing

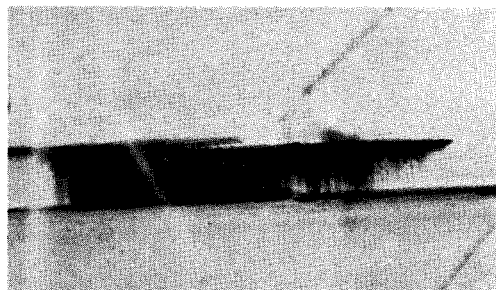


FIG. 6. Silver platelets electrically connected by a bundle of  $c$ -axis threads (magnification  $\times 202$ ).

<sup>22</sup> F. Feigl, *Spot Tests* (Nordemann Publishing Company, New York, 1937), pp. 13–14.

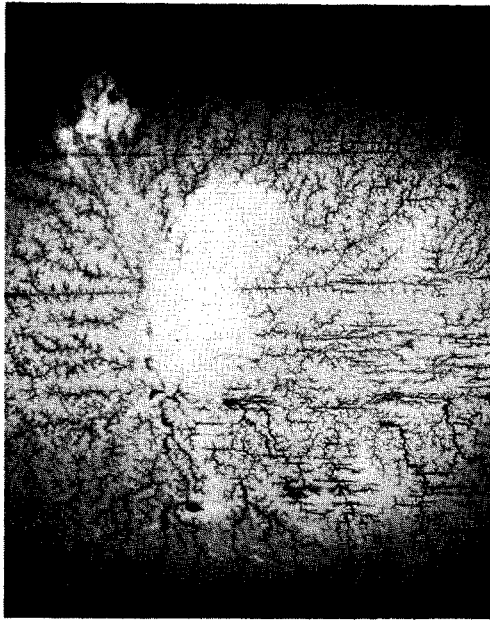


FIG. 7. Silver platelet and dendritic growth using synthetic quartz (magnification  $\times 32$ ).

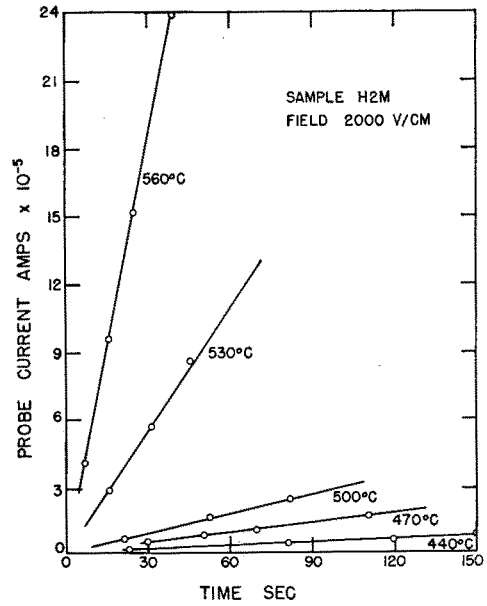


FIG. 9. Probe current vs time for various temperatures, using a silver center electrode. Probe potential  $-350$  V, minimum crystal thickness  $1.75$  mm.

from the basal plane. Evidence of lattice strain could be seen between crossed polaroids in samples sectioned and polished so as to expose the platelet edge. Although quartz is normally reported to fracture conchoidally, basal plane cleavage could be induced mechanically at a platelet-quartz interface.

With synthetic quartz, metallic "platelets" grew much more slowly in the basal plane, and usually lacked a symmetrical outline. In addition to the platelets, con-

siderable dendritic growth occurred as in Fig. 7, usually in spurts above  $500^\circ\text{C}$  for probes of minus 300 to 500 V. These growth spurts seemed to be accompanied by luminescence at the tips of some of the dendrites, and pulses of  $10^{12}$ – $10^{14}$  electron charges in the probe current.

Figures 8 and 9 show the dependence of typical Ag platelet diameter and probe current upon time for several temperatures. Both plots are linear with time for platelet diameters greater than about  $10^{-2}$  cm. For

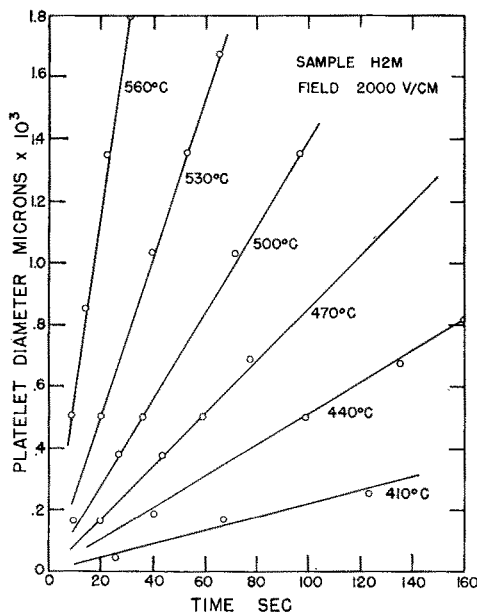


FIG. 8. Silver platelet growth for various temperatures. Probe potential  $-350$  V, minimum crystal thickness  $1.75$  mm.

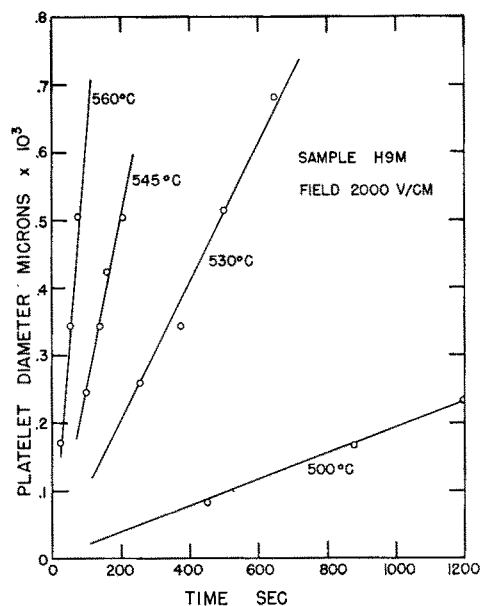


FIG. 10. Gold platelet growth rates for various temperatures. Probe potential  $-400$  V, minimum crystal thickness  $2.00$  mm.

smaller platelets the data were nonreproducible, and appeared to depend, *inter alia*, upon the prior length of time the charged probe had remained in the vicinity before actually making contact with quartz. It was supposed that the effective moment of electrical contact was slightly uncertain, and the linear curves of Figs. 8 and 9 have therefore been shifted in time (by less than 20 sec) so as to pass through the origin. Transients were seen, similar to the displacement currents.<sup>1</sup> At 560°C and 510 V the initial half-life was less than 1 sec. As the transient decayed its half-life increased manifold. Au behaved qualitatively similarly to Ag in all respects studied. Typical platelet growth data are shown in Fig. 10. Ag and Au platelet growth rate is shown as a function of temperature in Fig. 11 for different calculated

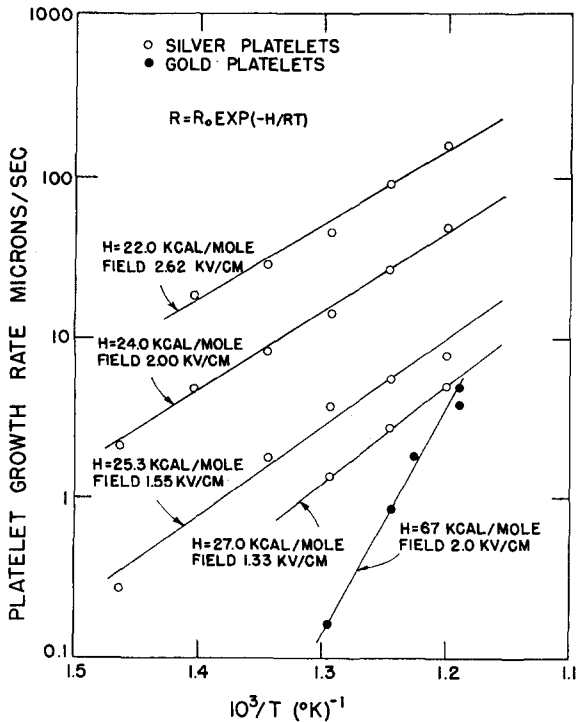


FIG. 11. Platelet growth rate vs reciprocal absolute temperature for various electric field strengths.

field strengths (using applied potential and measured platelet distances). Activation energies  $H$  obtained from slopes in Fig. 11 are plotted against the square root of field strength ( $\mathcal{E}$ ) in Fig. 12. The value obtained on tests with Ag coated flat quartz plates is also shown. These fall near the straight line

$$H = H_0 - \beta(\mathcal{E})^{1/2}, \quad (1)$$

where  $H_0 = 38$  kcal/mole, and  $\beta = 0.32$  kcal [mole/(V/cm)<sup>1/2</sup>]. Hence the platelet radius  $r$  is approximately

$$r = Rt \exp[-(H_0 - \beta(\mathcal{E})^{1/2})/KT], \quad (2)$$

where  $R$  is a constant. No prominent surge current or visible phenomena were noted for either natural or

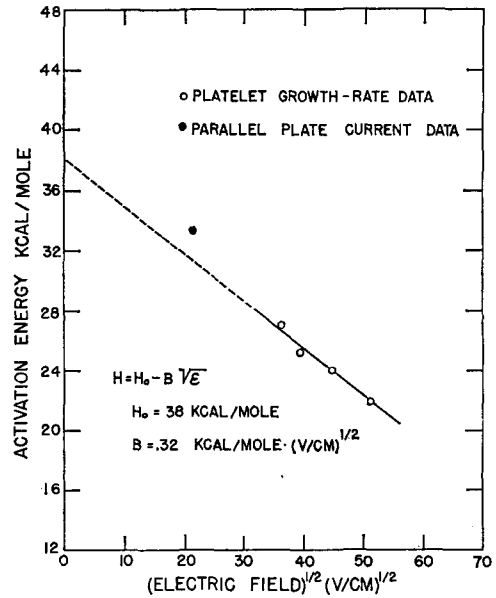


FIG. 12. Silver platelet growth-rate activation energies vs the square root of the electric field.

synthetic quartz for equatorial currents using Ag or Au anodes, and none were observed for axial currents using a steel anode. Activation energies were near 38 and 39 kcal/mole for equatorial and axial currents, respectively, as seen in Fig. 13. Considerably greater scatter occurred in the data for the probe current. The results, however, were similar to those above.

Transport of Na, Sn, Pb, Bi, and Pt was also qualitatively explored at 560°C in Madagascar quartz, with a probe of minus 400 V, but no platelet growth was

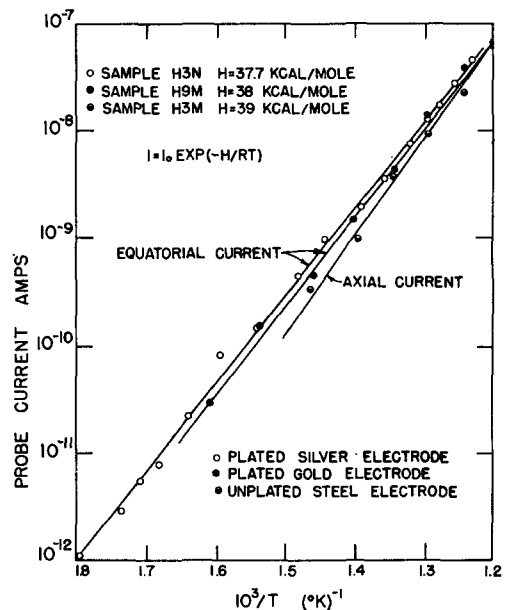


FIG. 13. Probe current vs reciprocal absolute temperature. Field about 2000 V/cm.

obvious. Na appeared to pass more easily than Ag (currents of the order of  $10^{-3}$  A), however, it oxidized on emergence and formed a considerable "blob" about the probe. It is uncertain whether any Sn, Pb, or Bi actually passed through the crystal ( $10^{-7}$ – $10^{-8}$  A currents). In all, one uncertain visible spot might have been formed (and promptly oxidized) with Pb, 3 with the Bi, and none with Sn. No geometric patterns were seen with Na, Sn, Pb, Bi, or a steel rod as anode. Pt produced several geometric patterns 10–20  $\mu$  in diameter and nothing else.

### DISCUSSION

Present work confirms the easier transport of impurity along the  $c$  axis. This is geometrically plausible<sup>1</sup> in a hard sphere model of the lattice (using Pauling's radii<sup>23</sup>), where the least constricted ( $\sim 0.6$  Å) path between adjacent interstitial positions follows the  $c$  axis.

The smaller singly charged ions tended to migrate more readily than the larger ones (except<sup>5</sup> possibly for Cu). Migration was not confirmed for any of the commonly multicharged ions. According to Faraday's law, the thickness  $S$  of an equivalent uniform circular platelet of Ag deposited by a current  $I$  can be calculated:

$$S = A \int I(t) dt / (\pi r^2 e z N_0 \rho) = 0.17 \pm 0.04 \mu \quad (3)$$

independent of temperature, where  $e z$  is the ionic charge,  $A$  is the atomic weight,  $\rho$  the density,  $N_0$  Avogadro's number, and numerical values for  $I$  and  $r$  from the data of Figs. 8 and 9 have been used. Comparison with the observed thicknesses of 0.3–0.5  $\mu$  implies (since the calculated thickness is less than the observed thickness) that probably the conduction current is purely ionic Ag. A problem concerning the mechanism of platelet formation arises from the experimental fact that the platelets formed within the bulk of the lattice have a nearly uniform thickness. The question is now this: If it is assumed that the metallic ions move along the  $c$ -axis channels, as has been amply demonstrated, it is not immediately clear why only a discrete platelet was formed, and why it was not thickest in the vicinity of the probe (where the transport could have occurred for a longer period of time), thinning out near the edges. This seems to indicate that the transport of ions takes place principally at the periphery of the platelet. This was further substantiated by the fact that both the probe current and platelet diameter increased linearly with time, hence the ion current would be proportional to the platelet diameter or circumference.

Consider the metallic ions that move along channels that intersect the plane of the platelet one or two lattice spaces from the platelet edge. Since axial motion of the

particles is considerably easier than equatorial motion, as was demonstrated, the particles eventually reach the plane of the platelet, but do not make electrical contact. However, as a result of the platelet being very thin, approximately 0.17  $\mu$ , there is a large electric field in the vicinity of the platelet edge. It is possible that this field, about  $10^7$  V/cm, acting over a distance of about a lattice space causes equatorial transport in the plane of the platelet. There may also be "free surface" in the form of a small crack preceding the platelet as it grows. The ions moving in this manner around the entire periphery form an expanding conducting metallic platelet. Ions moving along channels which are connected directly with the metallic platelet become neutralized on making electrical contact with the platelet, and remain lodged in their respective channels. They may also make occasional jumps in the equatorial direction. As time increases these channels continue to accept and hold the metallic impurities and thus broaden to form  $c$ -axis threads as seen in Fig. 5. The fact that the crystal fractures is not surprising when the proposed mechanism is considered. It is assumed that the metallic ion impurities migrate, interstitially, under the influence of the electric field, along the  $c$ -axis channels. As a result of the strain induced by the accumulative introduction of impurities, the formation and expansion of platelets, the crystal sometimes fractures, thus alleviating the strain.

An explanation concerning the differences observed for platelet formation in natural and synthetic quartz now seems plausible. The presence of numerous imperfections in synthetic quartz as compared to natural quartz has been shown through the study of resonator characteristics.<sup>14</sup> These imperfections were assumed to be interstitial and substitutional impurities, misalignment of the lattice due to broken silicon oxygen bonds, etc.

It is suggested that the dendritic type of growth of platelets in synthetic quartz, Fig. 7, is a result of the blocking or partially blocking of the  $c$ -axis channels by the above-mentioned imperfections. The subsequent behavior of the sporadic lengthening of the dendrite with an associated current pulse would represent the clearing out of a blocked channel or group of channels with a surge of silver ions arriving at the surface.

The mechanism which limits the rate at which metallic ions, under the influence of an electric field, migrate through the quartz lattice is of prime importance. The gross factors which are most likely to influence the rate of transport are: (1) motion of metallic ions from an external source into the crystal lattice; (2) migration of the metallic impurity ions through the crystal bulk; (3) nucleation or neutralization of the ions at or near the collecting electrode. In studying the diffusion of  $\text{Li}^+$  ion through quartz in an electric field, Vogel and Gibson<sup>5</sup> found that the diffusion process was independent of crystal thickness. In the current study similar results were noted while observing Ag platelet formation.<sup>16</sup>

<sup>23</sup> Charles Kittel, *Introduction to Solid State Physics* (John Wiley & Sons, Inc., New York, 1953), 2nd ed., p. 82.

Hence it seems doubtful that, at least, for Li and Ag that the field dependent rate limiting process is due to the migration of the ions through the bulk.

Concerning the energy of formation for internal surfaces through platelet growth, a theoretical calculation<sup>16</sup> following Gilman<sup>24</sup> yielded an energy of  $\sim 14.1$  kcal/mole (of surface). The presence of mobile  $\text{Ag}^+$  ions may reduce this value further. Comparison with 38 kcal/mole for platelet formation (extrapolated to zero field) suggests that this is probably not the rate limiting process.

<sup>24</sup> J. J. Gilman, *J. Appl. Phys.* **31**, 2208 (1960).

Moreover, it is not obvious how the field dependence would come about.

Hence it seems probable that the practical rate limiting factor for ions moving to the platelet edge is connected with a field dependent process of introducing metallic ions from an external source into the lattice. The current is "shut off" by other very high activation energies for flow other than to the platelet edge. An analysis of impurity introduction has been made elsewhere.<sup>25</sup>

<sup>25</sup> E. A. Milne, Jr., and P. Gibbs (to be published).

## Optical Maser Characteristics of Rare-Earth Ions in Crystals

L. F. JOHNSON

*Bell Telephone Laboratories, Incorporated, Murray Hill, New Jersey*

(Received 22 October 1962)

Several divalent and trivalent rare-earth ions incorporated in various host crystals have been found to exhibit stimulated emission in the near infrared. A report is presented describing some of the basic characteristics of these materials: absorption and fluorescence spectra, energy level diagrams, optical maser wavelengths and operating temperatures, and thresholds for stimulated emission. Recent observations on the  $\text{CaWO}_4:\text{Nd}^{3+}$  optical maser in continuous operation are also described.

SINCE the Schawlow-Townes<sup>1</sup> proposal extending the maser concept to the infrared and optical regions, the optical maser has become a practical reality. The predictions of this theory were first verified in ruby<sup>2,3</sup> ( $\text{Cr}^{3+}$  ions in  $\text{Al}_2\text{O}_3$ ). Optical maser action was then observed from  $\text{Sm}^{2+}$  ions in  $\text{CaF}_2$ ,<sup>4,5</sup>  $\text{U}^{3+}$  ions in  $\text{CaF}_2$ ,<sup>6</sup> and in He-Ne gas.<sup>7</sup>

During the past year or so, optical maser action has been observed in a number of systems incorporating divalent and trivalent rare-earth ions as active agents. The purpose of this paper is to present the results of a series of experiments, covering spectroscopic measurements and observations on optical maser behavior, on crystals of this type. The largest body of information concerns crystals containing the trivalent rare-earth ions  $\text{Nd}^{3+}$ ,  $\text{Ho}^{3+}$ , and  $\text{Tm}^{3+}$ . In particular,  $\text{Nd}^{3+}$  in  $\text{CaWO}_4$  is considered in some detail, and is discussed in two parts. Spectroscopic data related to maser operation is presented in Sec. II, along with similar data on

crystals containing  $\text{Ho}^{3+}$  and  $\text{Tm}^{3+}$ . The technical aspects of maser behavior is treated in Sec. V.

### I. EXPERIMENTAL

Fluorescence spectra were recorded by a PbS detector in conjunction with a Perkin-Elmer model 12G grating spectrometer. Emission was excited by either an Osram HBO 200 high-pressure mercury lamp or a 1000-W General Electric AH6 mercury lamp. Spectra at low temperature were obtained by inserting a crystal into a small quartz Dewar containing liquid nitrogen or hydrogen.

Optical maser spectral characteristics under pulse-illumination conditions were determined in the following manner. Single-crystal boules were cut and ground into cylindrical rods, typically 0.12 in. in diameter and 2 in. long, and both ends polished. Silver was evaporated onto the end surfaces, one end being left partially transmitting ( $< 1\%$ ). The rod was attached to one end of a hollow Cu-Ni tube, a glass window was cemented to the other end, and the assembly was placed inside a quartz Dewar. The Dewar was centered in a GE FT524 helical xenon flash lamp. The lamp was flashed by discharging an appropriate condenser (2 to 200  $\mu\text{F}$ ) charged typically to 1 kV. Light emerging from the lightly silvered end of the rod and passing up through the tube was focused onto the entrance slit of the spectrometer. Either an RCA 7102 photomultiplier tube or a cooled gold-doped germanium detector was employed

<sup>1</sup> A. L. Schawlow and C. H. Townes, *Phys. Rev.* **112**, 1940 (1958).

<sup>2</sup> T. H. Maiman, *Nature* **187**, 493 (1960).

<sup>3</sup> R. J. Collins, D. F. Nelson, A. L. Schawlow, W. Bond, C. G. B. Garrett, and W. Kaiser, *Phys. Rev. Letters* **5**, 303 (1960).

<sup>4</sup> P. P. Sorokin and M. J. Stevenson, *IBM J. Res. Develop.* **5**, 56 (1961).

<sup>5</sup> W. Kaiser, C. G. B. Garrett, and D. L. Wood, *Phys. Rev.* **123**, 766 (1961).

<sup>6</sup> P. P. Sorokin and M. J. Stevenson, *Phys. Rev. Letters* **5**, 557 (1960).

<sup>7</sup> A. Javan, W. R. Bennett, Jr., and D. R. Herriott, *Phys. Rev. Letters* **6**, 106 (1961).